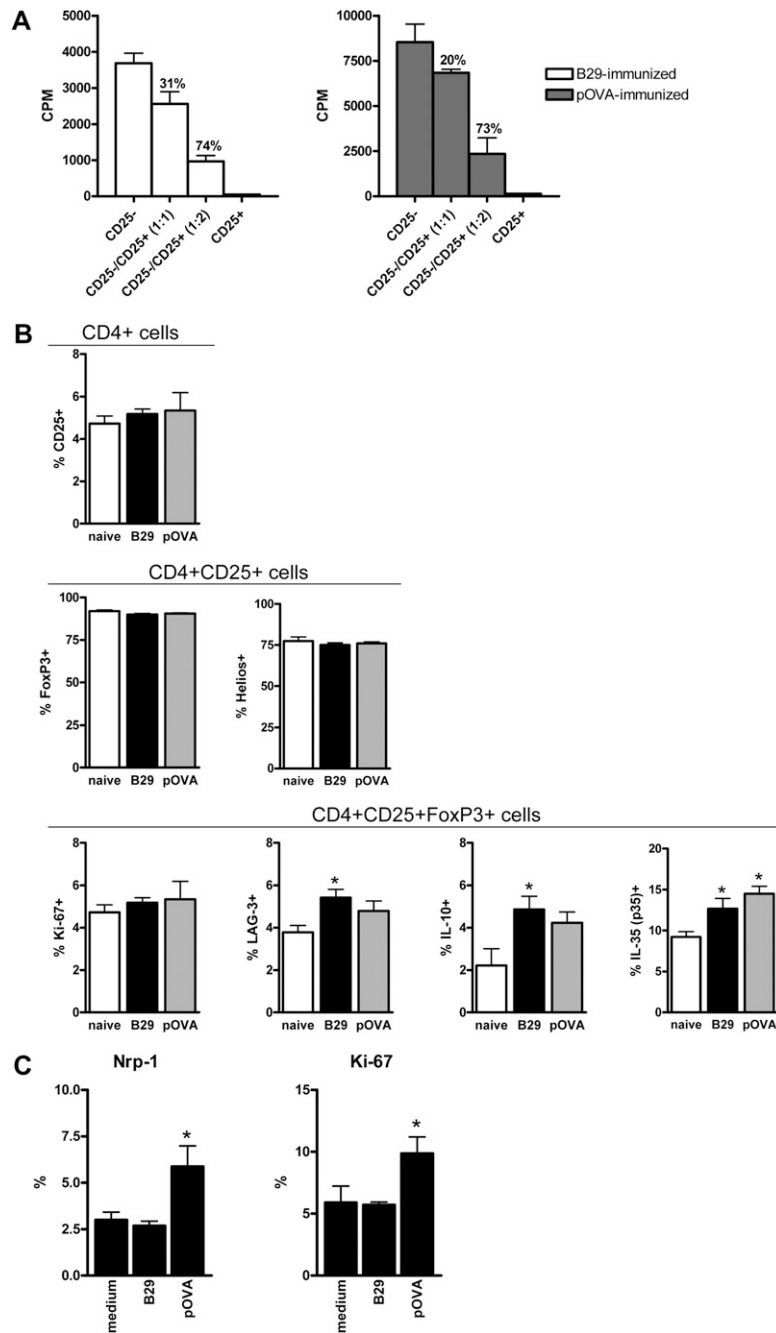
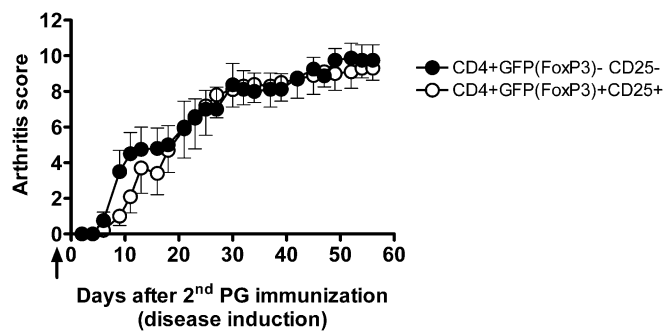


# Supporting Information

van Herwijnen et al. 10.1073/pnas.1206803109



**Fig. S1.** In vitro and phenotypic characterization CD4<sup>+</sup>CD25<sup>+</sup> T cells from B29- or pOVA-immunized mice. (A) CD4<sup>+</sup>CD25<sup>+</sup> and CD4<sup>+</sup>CD25<sup>-</sup> cells from B29- or pOVA-immunized mice were cocultured and stimulated by soluble anti-CD3 antibody. Data are mean of triplicate samples, and results are representative of two independent experiments. Percentages represent suppression of proliferation compared to CD4<sup>+</sup>CD25<sup>-</sup> cells alone. (B) Mice were immunized with B29 or pOVA and CD4<sup>+</sup>CD25<sup>+</sup> (FoxP3<sup>+</sup>) Tregs were analyzed by flow cytometry. Expression ( $\pm$ SEM) of markers related to Treg function were analyzed and showed enhanced expression of LAG-3, IL-10, and p35 (IL-35 subunit) in CD4<sup>+</sup>CD25<sup>+</sup>FoxP3<sup>+</sup> cells. *P* values are from an unpaired two-tailed Student *t* test in which Tregs from B29- or pOVA-immunized mice were compared with Tregs from naive mice. \**P* < 0.05; \*\*\**P* < 0.001. Data are mean of 5–10 animals per group, and data shown are representative of two independent experiments. (C) Splenocytes from pOVA-immunized mice were restimulated for 24 h in the presence of B29 or pOVA and stained for Ki-67 (Right) and Nrp-1 (Left). Percentage of positive cells ( $\pm$ SEM) is shown within the CD4<sup>+</sup>CD25<sup>+</sup>FoxP3<sup>+</sup> population. *P* values are from an unpaired two-tailed Student *t* test in which pOVA was compared with B29. \**P* < 0.05. Data are mean of 5–10 animals per group and are representative of two independent experiments.



**Fig. S2.** CD4+CD25+FoxP3+ T cells from pOVA-immunized donors are not suppressive in vivo. Mean arthritis scores ( $\pm$ SEM) of recipients with PGIA after adoptive transfer. One day before the second PG immunization, animals received  $3 \times 10^5$  CD4<sup>+</sup> cells i.v. from pOVA-immunized FoxP3–GFP reporter donor mice (arrow). Donor CD4<sup>+</sup> cells were selected on expression of CD25 and/or GFP (FoxP3). [CD4<sup>+</sup>GFP(FoxP3)<sup>–</sup>CD25<sup>–</sup>,  $n = 5$ ; CD4<sup>+</sup>GFP(FoxP3)<sup>+</sup>CD25<sup>+</sup>,  $n = 4$ ].

**Table S1. Identification of *Mt*-Hsp70 epitopes**

Pool	Peptide name	Sequence	Position
I	B18	YTAPEISARILMKLK	86–100
	B59	KPFQSVIADTGISVS	291–305
	B107	AEGGSKVPEDTLNKV	530–544
	B108	AQAASQATGAHPGG	585–599
II	B7	EGSRTPSIVAFARN	31–45
	B47	MQRLREAAEKAKIEL	231–245
	B67	GGKEPNKGVNPDEVV	331–345
	B69	DEVVAVGAALQAGVL	342–356
	B74	LDVTPLSLGIETKGG	366–380
III	B29	VLRIVNEPTAAALAY	141–155
	B34	ILVFDLGGGTFDVSL	166–180
	B89	RGIPQIEVTFDIDAN	441–455
	B90	QIEVTFDIDANGIVH	445–459

To identify the dominant T-cell epitopes of Mt Hsp70, mice were immunized on days 0 and 14 with Mt Hsp70 in DDA. On day 28, spleen cells were isolated and restimulated with a panel of 123 overlapping 15-mer peptides covering the complete sequence of Mt Hsp70. Subsequently induced T-cell responses were detected by <sup>3</sup>H-thymidine incorporation. In multiple experiments the 13 peptides depicted repeatedly induced proliferation upon in vitro restimulation with the peptides and were therefore selected as dominant epitopes. The peptides were divided into three pools according to the degree of sequence identity with mouse Hsp70-peptides: nonidentical (pool I), moderately identical (pool II), or highly identical (pool III).

**Table S2. Origin and sequence of highly conserved B29 peptides**

Peptide	Protein	Origin	ID	Sequence
B29	DnaK (Hsp70)	<i>Mycobacterium tuberculosis</i>	885946	VLRIVNEPTAAALAY
mB29a <sup>†</sup>	HspA9	<i>Mus musculus</i>	15526	VLR <b>V</b> INEPTAAALAY
	(GRP75)	<i>Homo sapiens</i>	3313	VLR <b>V</b> INEPTAAALAY
mB29b <sup>†</sup>	HspA1A	<i>Mus musculus</i>	193740	VLR <b>I</b> INEPTAA <b>A</b> IAY
	(Hsp72)	<i>Homo sapiens</i>	3303	VLR <b>I</b> INEPTAA <b>A</b> IAY
	HspA8	<i>Mus musculus</i>	15481	VLR <b>I</b> INEPTAA <b>A</b> IAY
	(Hsc70)	<i>Homo sapiens</i>	3312	VLR <b>I</b> INEPTAA <b>A</b> IAY

Human and mouse peptides of the same protein were completely identical. Altered residues compared with *Mycobacterium tuberculosis* are in bold and underlined. ID, GeneID in the National Center for Biotechnology Information (NCBI) Entrez Gene database ([www.ncbi.nlm.nih.gov/entrez/query.fcgi?db=gene](http://www.ncbi.nlm.nih.gov/entrez/query.fcgi?db=gene)).

<sup>†</sup>mB29a and mB29b are mammalian homologs of mycobacterial Hsp70 peptide B29.

**Table S3. Hsp70 is a major contributor to the MHC class II ligandome**

Sequence	Class II type	MHC origin	Protein source (100% ID)	Entrez gene ID	Ref.
QQYLPLPTPKVIGID	HLA-DR10 (DRB1*1001)	Human	HSPA13 (23–37)	6782	1
IIANDQGNRTTPSY	I-Ak	Mouse	HSPA8 (28–41)	15481	2
			HSPA2 (29–42)	15512	
			HSPA1L (30–43)	15482	
			HSPA1A (28–41)	193740	
			HSPA1B (28–41)	15511	
ITPSYVAFTPEGERL	I-Ab	Mouse	HSPA5 (62–76)	14828	3
TPSYVAFTDTERLIG (DA)	HLA-DR7	Human	HSPA8 (38–52)	3312	4
			HSPA2 (39–53)	3306	
			HSPA1L (40–54)	3305	
			HSPA1A (38–52)	3303	
TPSYVAFTDTERLIGD	HLA-DQ2	Human	As above	As above	5
DVYVGYESVELADSNPQ	HLA-DQ2	Human	HSPA13 (77–93)	6782	5
DAAKNQLTSNPEN	I-Ag7	Mouse	HSPA5 (79–91)	14828	6
NPTNTVFDKRLIGRRFD	HLA-DRB1*1104	Human	HSPA8 (62–79)	3312	7
QDIKFLPFKVVKKTKPY	BoLA-DRB3*1201 (in mus line)	Bovine	HSPA5 (111–128)	14828	8
<b>LNVLRIINEPTAAAIAYG</b> <b>(NVLRIINEPTAAAIAYG)</b>	HLA-DRB1*0401 (in rat line)	Human	HSPA8 (167–184)	24468	9
			HSPA1A (167–184)	24472	
			HSPA1L (169–186)	24963	
			HSPA2 (168–185)	60460	
<b>NVLRIINEPTAAAIAYG</b>	HLA-DRB1*0401/DRB4*0101	Human	HSPA8 (168–184)	3312	10
			HSPA1A (168–184)	3303	
			HSPA1L (170–186)	3305	
			HSPA2 (169–185)	3306	
			HSPA6 (170–186)	3310	
<b>NVLRIINEPTAAAIAYG</b>	DRB1*0401/*02x/DRB5*0101	Human	HSPA8 (168–184)	3312	11
			HSPA1A (168–184)	3303	
			HSPA1L (170–186)	3305	
			HSPA2 (169–185)	3306	
			HSPA6 (170–186)	3310	
<b>NVMRIINEPTAAAIAYG</b>	DRB1*0401/*02x/DRB5*0101	Human	HSPA5 (194–210)	3309	11
<b>VMRIINEPTAAAIAYG</b>	HLA-DRB1*0401/DRB4*0101	Human	HSPA5 (195–210)	3309	10
<b>IINEPTAAAIAYGLD</b>	HLA-DQ6 (B*602)	Human	HSPA8 (172–186)	3312	12
			HSPA2 (173–187)	3306	
			HSPA1L (174–188)	3305	
			HSPA1A (172–186)	3303	
			HSPA5 (198–212)	3309	
FDVSILTIEDGIFE	HLA-DQ2	Human	HSPA8 (205–218)	3312	5
NRMVNHFAEFKRK	I-Ek	Mouse	HSPA8 (236–249)	15481	13
RMVNHFAEFKRKH	I-Ek	Mouse	HSPA8 (236–249)	15481	14
VNHFAEFKRKHKKD	HLA-DR11/w52	Human	HSPA8 (238–252)	3312	15
XDFYTSITRAXFEE	HLA-DR11/w52	Human	HSPA8 (291–304)	3312	15
			HSPA1A (291–304)	3303	
			HSPA1L (293–306)	3305	
			HSPA2 (294–307)	3306	
			HSPA6 (294–306)	3310	
EGEDFSETLTRAKFEEL	BoLA-DRB3*1201(in mus line)	Bovine	HSPA5 (315–331)	14828	8
ADLFRGTLDPVEK	HLA-DQ6 (B*0604)	Human	HSPA8 (307–319)	3312	12
KSINPDEAVAYG	HLA-DQ2	Human	HSPA8 (361–372)	3312	5
			HSPA1A (361–372)	3303	
			HSPA1L (363–374)	3305	
			HSPA2 (364–375)	3306	
			HSPA6 (363–374)	3310	
			HSPA8 (361–372)	3312	
TIPTKQTQFTTYSNDQP	RT1.BI	Rat	HSPA8 (419–436)	24468	16
			HSPA1A (419–436)	24472	
VPTKKSQIFSTASDNQPTVT	HLA-DRB1*0401/DRB4*0101	Human	HSPA5 (443–462)	3309	10
GERAMTKDNNLLG	HLA-DR4Dw4	Human	HSPA8 (445–457)	3312	17
			HSPA1A (445–457)	3303	
			HSPA1L (447–459)	3305	
			HSPA2 (448–460)	3306	
			HSPA6 (447–459)	3310	

**Table S3. Cont.**

Sequence	Class II type	MHC origin	Protein source (100% ID)	Entrez gene ID	Ref.
GERAMTKDNNLLGKFE	HLA-DRB1*0401/DRB4*0101	Human	HSPA8 (445–460) HSPA1A (445–460)	3312 3303	10
GERAMTKDNNLLGRFE	HLA-DRB1*0401/DRB4*0101	Human	HSPA6 (447–462)	3310	10
ANGILNVSAVDKSTGKE	HLA-DRB*0401	Human	HSPA8 (482–499)	3312	18
GILNVSAVDKSTGK	HLA-DRB*0401	Human	HSPA8 (484–497)	3312	18
GILNVSAVDKSTGKE	HLA-DRB1*0401/DRB4*0101	Human	HSPA8 (484–498)	3312	10
CNEIINWLDKNQ	HLA-DR4Dw10	Human	HSPA8 (574–585)	3312	17
ISWLDKNQTAEKEEFE	HLA-DQ8 (transgenic in NOD)	Human	HSPA8 (578–593)	15481	6
YSGGGPPTGEEDTSEKDEL	I-Ag7	Mouse	HSPA5 (636–655)	14828	6

The Hsp70 nomenclature is as proposed by Kampinga et al. (19). Published data of Hsp70 sequences found in MHC class II are shown. The sequence of B29 and its endogenous homologs were frequently eluted from different MHC class II molecules. Peptides are listed according to sequence number. Bold indicates peptides homologous to B29. In the boxed section B29 homolog peptides eluted from RA associated HLA-DRB1\*0401.

- Alvarez I, et al. (2008) The rheumatoid arthritis-associated allele HLA-DR10 (DRB1\*1001) shares part of its repertoire with HLA-DR1 (DRB1\*0101) and HLA-DR4 (DRB\*0401). *Arthritis Rheum* 58:1630–1639.
- Nelson CA, Roof RV, McCourt DW, Unanue ER (1992) Identification of the naturally processed form of hen egg white lysozyme bound to the murine major histocompatibility complex class II molecule I-Ak. *Proc Natl Acad Sci USA* 89:7380–7383.
- Dongre AR, et al. (2001) In vivo MHC class II presentation of cytosolic proteins revealed by rapid automated tandem mass spectrometry and functional analyses. *Eur J Immunol* 31:1485–1494.
- Chicz RM, et al. (1993) Specificity and promiscuity among naturally processed peptides bound to HLA-DR alleles. *J Exp Med* 178:27–47.
- Stepniak D, et al. (2008) Large-scale characterization of natural ligands explains the unique gluten-binding properties of HLA-DQ2. *J Immunol* 180:3268–3278.
- Suri A, Walters JJ, Gross ML, Unanue ER (2005) Natural peptides selected by diabetogenic DQ8 and murine I-A(g7) molecules show common sequence specificity. *J Clin Invest* 115:2268–2276.
- Verreck FA, et al. (1996) Natural peptides isolated from Gly86/Val86-containing variants of HLA-DR1, -DR11, -DR13, and -DR52. *Immunogenetics* 43:392–397.
- Sharif S, Mallard BA, Wilkie BN (2003) Characterization of naturally processed and presented peptides associated with bovine major histocompatibility complex (BoLA) class II DR molecules. *Anim Genet* 34:116–123.
- Muntasell A, et al. (2004) Dissection of the HLA-DR4 peptide repertoire in endocrine epithelial cells: Strong influence of invariant chain and HLA-DM expression on the nature of ligands. *J Immunol* 173:1085–1093.
- Dengjel J, et al. (2005) Autophagy promotes MHC class II presentation of peptides from intracellular source proteins. *Proc Natl Acad Sci USA* 102:7922–7927.
- Halder T, et al. (1997) Isolation of novel HLA-DR restricted potential tumor-associated antigens from the melanoma cell line FM3. *Cancer Res* 57:3238–3244.
- Sanjeevi CB, Lybrand TP, Stevanovic S, Rammensee HG (2002) Molecular modeling of eluted peptides from DQ6 molecules (DQB1\*0602 and DQB1\*0604) negatively and positively associated with type 1 diabetes. *Ann N Y Acad Sci* 958:317–320.
- Marrack P, Ignatowicz L, Kappler JW, Boymel J, Freed JH (1993) Comparison of peptides bound to spleen and thymus class II. *J Exp Med* 178:2173–2183.
- Freed JH, Marrs A, VanderWall J, Cohen PL, Eisenberg RA (2000) MHC class II-bound self peptides from autoimmune MRL/lpr mice reveal potential T cell epitopes for autoantibody production in murine systemic lupus erythematosus. *J Immunol* 164:4697–4705.
- Newcomb JR, Cresswell P (1993) Characterization of endogenous peptides bound to purified HLA-DR molecules and their absence from invariant chain-associated alpha beta dimers. *J Immunol* 150:499–507.
- Reizis B, et al. (1996) The peptide binding specificity of the MHC class II I-A molecule of the Lewis rat, RT1.B1. *Int Immunol* 8:1825–1832.
- Friede T, et al. (1996) Natural ligand motifs of closely related HLA-DR4 molecules predict features of rheumatoid arthritis associated peptides. *Biochim Biophys Acta* 1316:85–101.
- Lippolis JD, et al. (2002) Analysis of MHC class II antigen processing by quantitation of peptides that constitute nested sets. *J Immunol* 169:5089–5097.
- Kampinga HH, et al. (2009) Guidelines for the nomenclature of the human heat shock proteins. *Cell Stress Chaperones* 14:105–111.

**Table S4. MHC class II presented Hsp70 peptides eluted from in vitro cultured murine bone marrow-derived DCs**

Sequence	Relative abundance, %
VLRVIN	4
VLRVINE	4
VLRVINEP	13
VLRVINEPT	1
VLRVINEPTA	2
VLRVINEPTAA	9
VLRVINEPTAAA	6
VLRVINEPTAAAL	55
LRVINEPTAAAL	5
<b>Total</b>	<b>100</b>

Peptide–MHC complexes were isolated from BM-derived DCs. Subsequently, eluted peptides were analyzed by data-dependent nanoscale LC/MS. Several homologs of the mB29a peptide varying in length are depicted, and their relative abundance compared with all eluted mB29a variants is shown.